

Supporting information for

Improving Flame Retardancy of in-situ Silica-Epoxy Nano-composites cured with Aliphatic Hardener: Combined effect of DOPO-based flame-retardant and Melamine

Aurelio Bifulco^{1,2}, Dambarudhar Parida², Khalifah A. Salmeia^{2,3}, Sandro Lehner², Rolf Stämpfli⁴, Hilber Markus², Giulio Malucelli^{5,*}, Francesco Branda^{1,*}, Sabyasachi Gaan^{2,*}

¹*Department of Chemical Materials and Industrial Production Engineering (DICMaPI) University of Naples Federico II, Naples, Italy*

²*Laboratory for Advanced Fibers, Empa Swiss Federal Laboratories for Materials Science and Technology, Lerchenfeldstrasse 5, 9014 St. Gallen, Switzerland*

³*Department of Chemistry, Faculty of Science, Al-Balqa Applied University, 19117 Al-Salt, Jordan*

⁴*Laboratory for Biomimetic Membranes and Textiles, Empa Swiss Federal Laboratories for Materials Science and Technology, Lerchenfeldstrasse 5, 9014 St. Gallen, Switzerland*

⁵*Department of Applied Science and Technology, Politecnico di Torino, Viale Teresa Michel 5, Alessandria 15121, Turin, Italy*

*Corresponding authors E-mails: branda@unina.it, giulio.malucelli@polito.it,
sabyasachi.gaan@empa.ch

Table of contents

1. Synthesis of 6H-dibenz[c,e][1,2]oxaphosphorin,6-[(1-oxido-2,6,7-trioxa-1-phosphabicyclo[2.2.2]oct-4-yl)methoxy]-, 6-oxide (DP).....	3
2. ATR-FTIR spectroscopy	4
Fig. S1	4
3. Thermal analysis	5
Fig. S2	5
Table S1	5
4. Vertical flame spread tests	6
Fig. S3	6
5. Pyrolysis combustion flow calorimetry results.....	7
Table S2	7
6. Cone calorimetry tests	8
Fig. S4	8
7. Pyrolysis–Gas Chromatography–Mass and Direct Insertion Probe–Mass Spectrometry.	9
Table S3	9
Fig. S5	9
Fig. S6	10
Fig. S7	10
Table S4	11
Scheme S1	11
Table S5	12
8. Mechanical behavior	12
Table S6	12
References	13

1. Synthesis of 6H-dibenz[c,e][1,2]oxaphosphorin,6-[(1-oxido-2,6,7-trioxa-1-phosphabicyclo[2.2.2]oct-4-yl)methoxy]-, 6-oxide (DP)

DOPO (5.0 g, 23.1 mmol) was charged in a three-neck round bottomed flask connected to a condenser and N₂ inlet. Dry Toluene (50 mL) was added under nitrogen, followed by the addition of N-Chlorosuccinimide (NCS) (3.40 g, 25.4 mmol) in small portions via side arm under N₂ at ambient temperature. After complete addition, the reaction mixture was stirred at ambient temperature overnight. The white precipitates were removed by filtration under N₂ using Schlenk frit. The solvent was removed under vacuum. The residue was re-dissolved in dichloromethane (50 mL) and transferred under N₂ to a dropping funnel and was slowly added to a mixture of 1-oxo-4-hydroxymethyl-2,6,7-trioxa-1-phosphabicyclo [2.2.2]octane (PEPA) (4.17 g, 23.1 mmol) and triethylamine (2.80 g, 27.8 mmol) in dichloromethane (100 mL) at ambient temperature. The reaction was again kept under stirring overnight at ambient temperature. The solvent was then completely removed and ethanol (50 mL) was added while stirring, forming a white product. The product was then collected by filtration and washed with ethanol and dried in vacuum at 80 °C until constant weight (4.45 g, 50% yield). The NMR data fit well with the published reports [1, 2].

2. ATR-FTIR spectroscopy

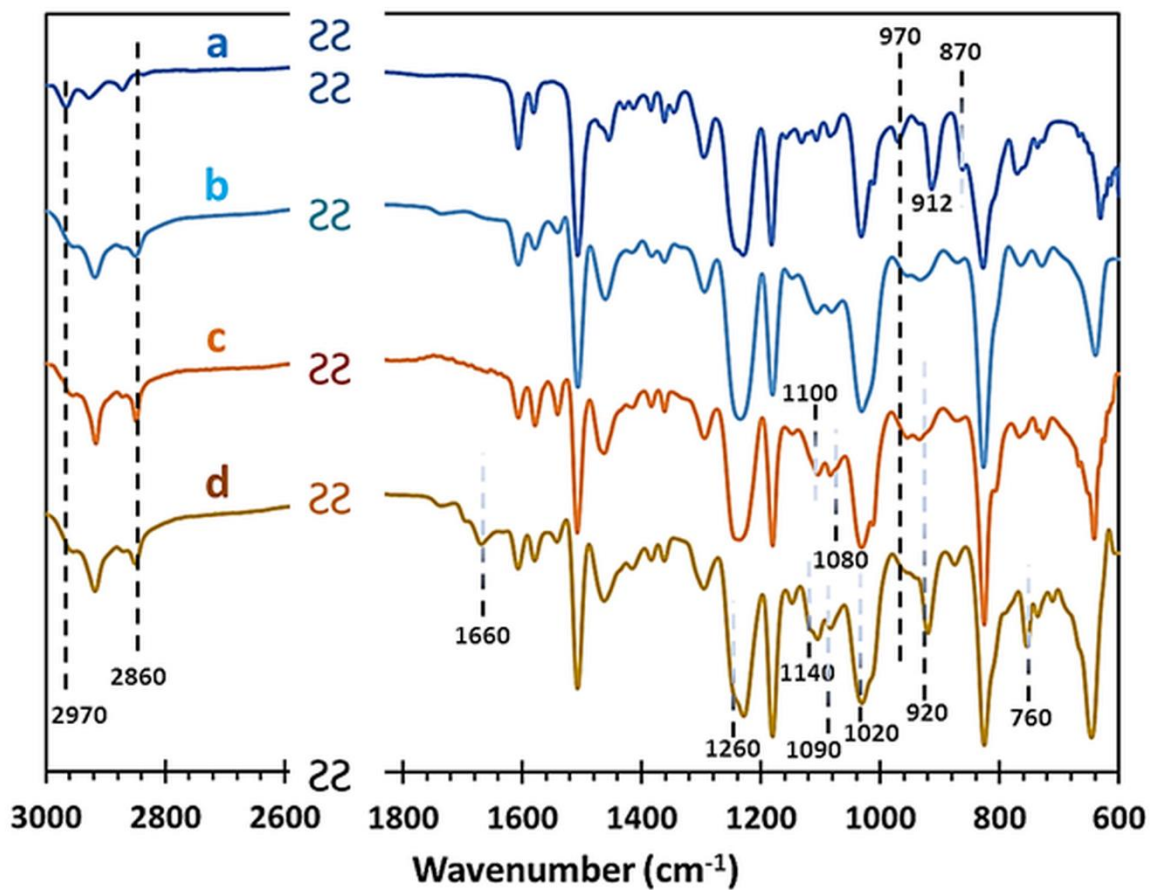


Fig. S1. ATR-FTIR spectra of the uncured resin **EPO_WH** (a), cured resin **EPO** (b), in-situ silica-epoxy system **EPO2Si** (c) and in-situ silica-epoxy system containing 2 wt.% of P and melamine **EPO2Si_DP2P_Mel** (d).

3. Thermal analysis

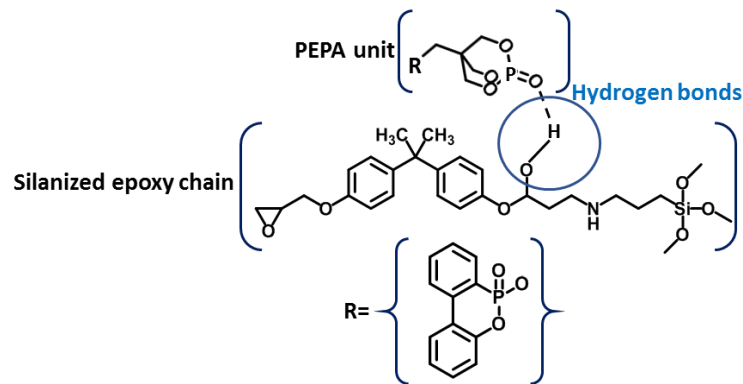


Fig. S2. Formation of hydrogen bonds between the oxygen of DP structure and hydroxyl groups, of the silanized epoxy chains, formed because of the cross-linking process [2-4].

Table S1. Thermogravimetry analysis (TGA) data collected in air and N₂ atmosphere for all the investigated samples. T_{5%} is the temperature, at which 5% weight loss was recorded. T_{max1}, T_{max2} and T_{max3} are the temperatures, at which the weight loss rate reaches the maximum; the residues at 800 °C and at the T_{max} temperatures are also reported.

Sample	T _{5%} (°C)	T _{max1} (°C)	T _{max2} (°C)	T _{max3} (°C)	Residue (wt.%) at 800 °C			
					T _{max1}	T _{max2}	T _{max3}	800 °C
<i>Under air</i>								
EPO	336	351	519	-	75	18	-	0.7
EPO_DP2P	266	308	356	535	77	58	35	13
EPO_Mel	259	269	349	514	92	71	24	1
EPO_DP2P_Mel	261	244	322	533	97	73	36	8
EPO2Si	293	367	553	-	61	11	-	1
EPO2Si_DP2P	255	187	322	535	98	69	34	11
EPO2Si_Mel	235	263	353	536	88	68	20	2
EPO2Si_DP2P_Mel	242	263	320	541	92	75	34	10
EPO2Si_DP1P_Mel	243	327	536	747	71	30	12	8
<i>Under N₂</i>								
EPO	338	354	-	-	73	-	-	8
EPO_DP2P	295	318	-	-	67	-	-	13
EPO_Mel	258	359	-	-	60	-	-	7
EPO_DP2P_Mel	333	358	-	-	74	-	-	12
EPO2Si	333	358	-	-	74	-	-	12
EPO2Si_DP2P	245	360	-	-	64	-	-	12
EPO2Si_Mel	270	324	-	-	70	-	-	12
EPO2Si_DP2P_Mel	250	366	-	-	56	-	-	9
EPO2Si_DP1P_Mel	338	354	-	-	74	-	-	8

4. Vertical flame spread tests

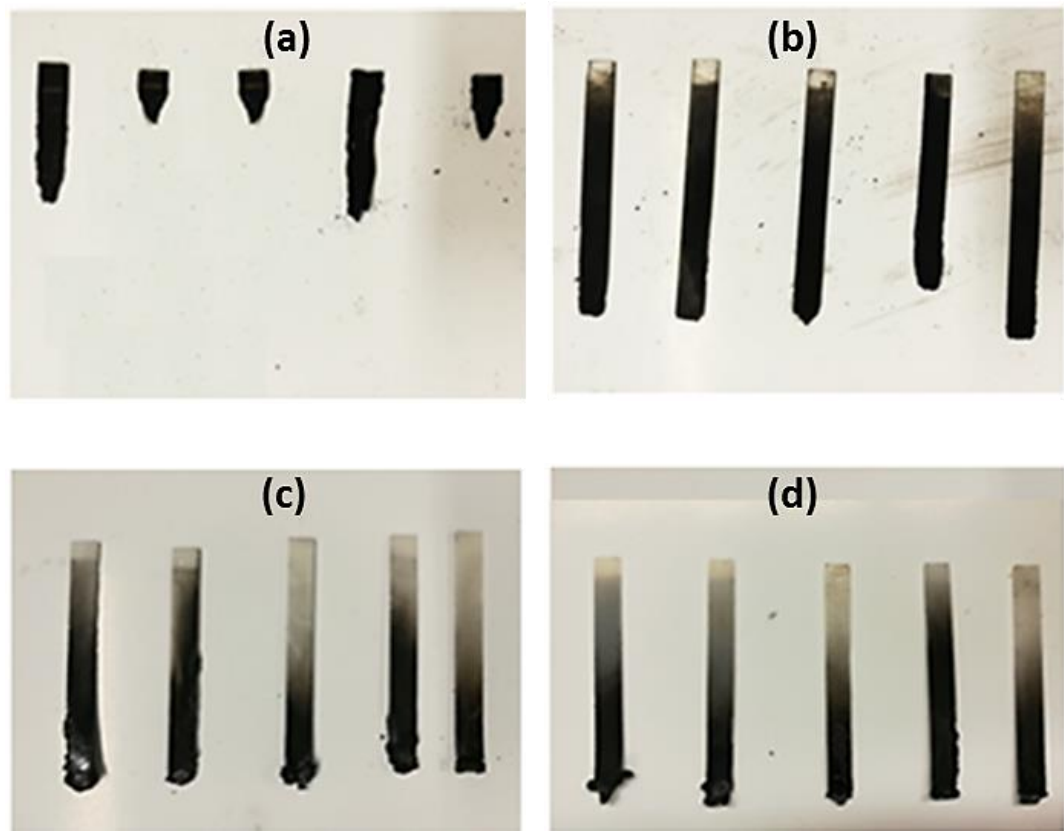


Fig. S3. Residues after UL-94 VB tests of (a) EPO, (b) EPO2Si, (c) EPO_DP2P_Mel and (d) EPO2Si_DP2P_Mel.

5. Pyrolysis combustion flow calorimetry results

Table S2. Pyrolysis Combustion Flow Calorimeter data for all the investigated samples.

Sample	THR (kJ/g)	HRC (J/g-K)	pHRR (W/g)	Residue (wt.%)
EPO	30 ± 0.3	539 ± 44	545 ± 57	6 ± 0.2
EPO_DP2P	24 ± 4	434 ± 99	371 ± 91	16 ± 0.3
EPO_Mel	24 ± 5	633 ± 165	494 ± 158	9 ± 3
EPO_DP2P_Mel	26 ± 1	334 ± 21	297 ± 14	7 ± 1
EPO2Si	28 ± 0.1	450 ± 24	448 ± 22	11 ± 1
EPO2Si_DP2P	24 ± 3	434 ± 99	372 ± 92	14 ± 2
EPO2Si_Mel	26 ± 1	462 ± 4	410 ± 8	11 ± 0.5
EPO2Si_DP2P_Mel	26 ± 1	316 ± 34	270 ± 38	15 ± 2
EPO2Si_DP1P_Mel	25 ± 0.1	367 ± 17	319 ± 24	10 ± 1

6. Cone calorimetry tests

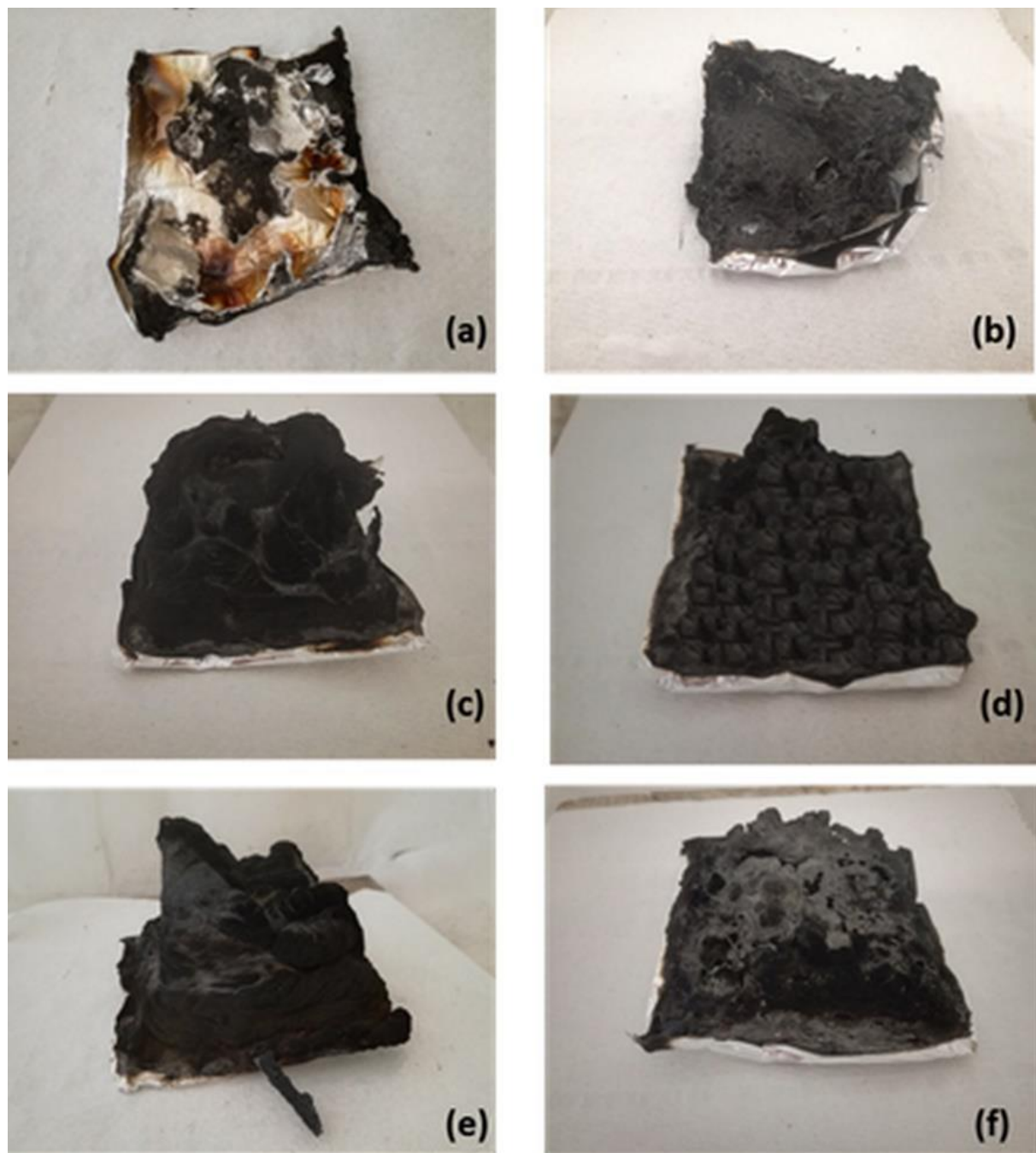
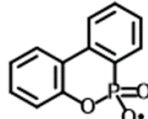
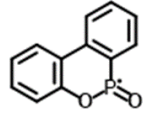
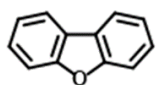
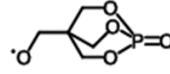
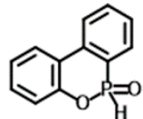


Fig. S4. Photographs of the char residues obtained after cone calorimetry tests for **EPO** (a), **EPO₂Si** (b), **EPO_DP2P** (c), **EPO_DP2P_Mel** (d), **EPO₂Si_DP2P** (e) and **EPO₂Si_DP2P_Mel** (f).

7. Pyrolysis–Gas Chromatography–Mass and Direct Insertion Probe–Mass Spectrometry.

Table S3. Major decomposition products of DP [2].

Compound	m/z	Symbol	Compound	m/z	Symbol
	231	R	PO^{\cdot}	47	V
	215	S		168	Z
	179	T			
	216	U			

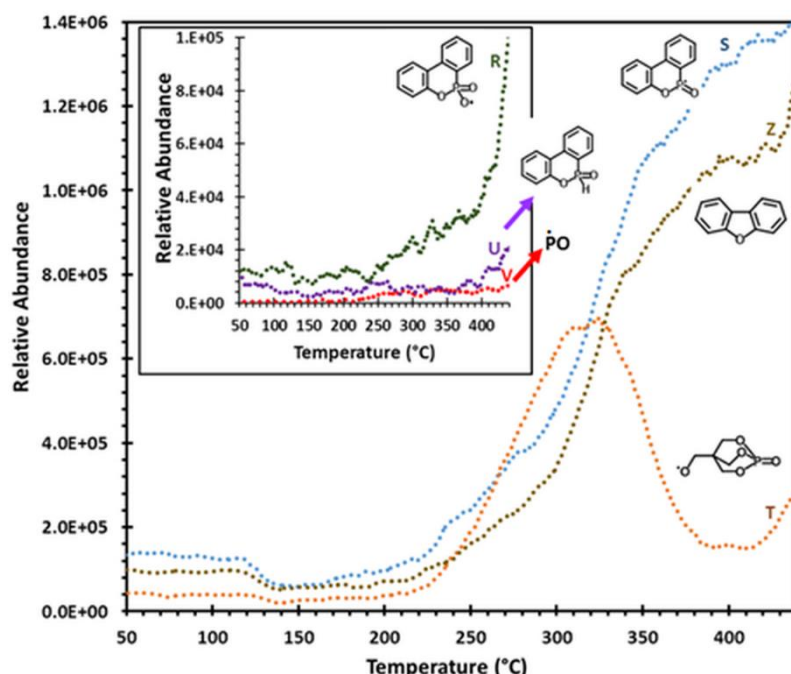


Fig. S5. DIP-MS analysis of EPO2Si_DP2P_MeI; thermograms of its major decomposition species listed in Table S3 are shown in the inset.

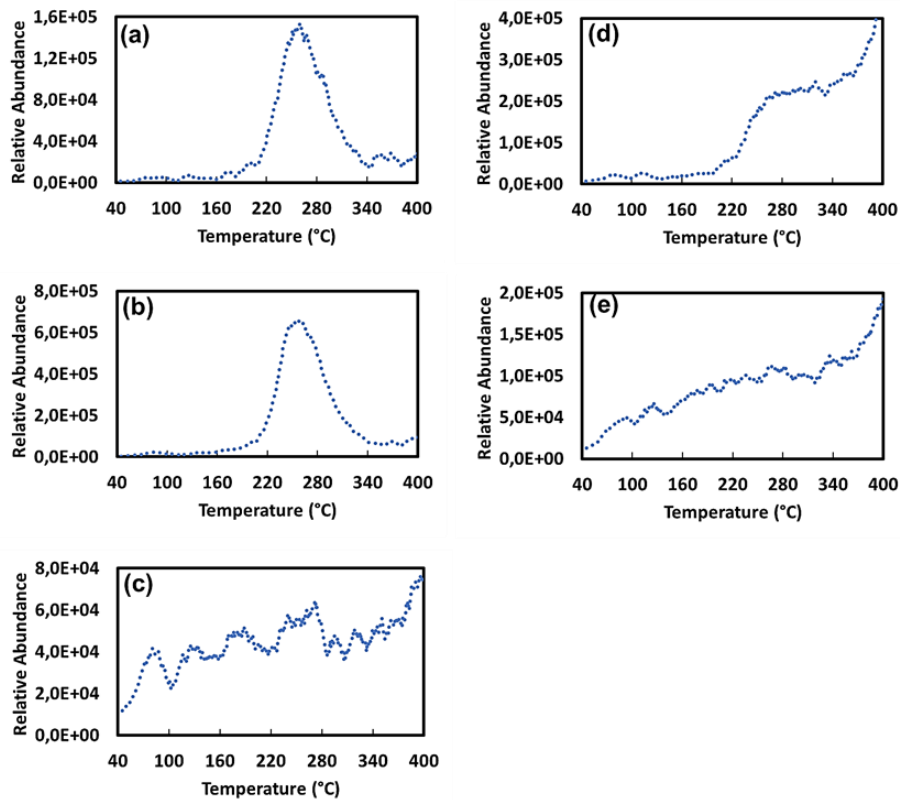


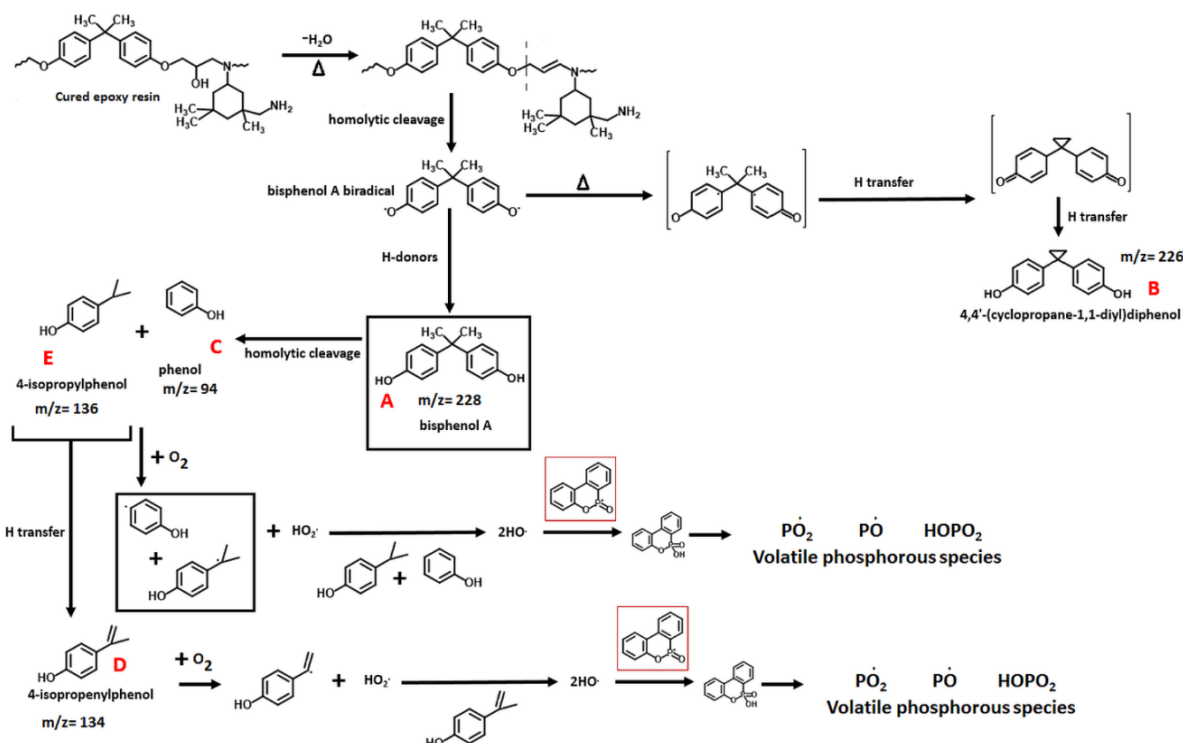
Fig. S6. DIP-MS analysis of EPO, thermograms its major decomposition species listed in Table S4: bisphenol A (a), 4,4'-(cyclopropane-1,1-diyl)diphenol (b), phenol (c), 4-isopropenylphenol (d), 4-isopropylphenol (e).



Fig. S7. Intumescence char residue after cone calorimetry test for **EPO2Si_DP2P_Mel** [5, 6].

Table S4. Major decomposition products of pristine epoxy with cycloaliphatic hardener under N₂ atmosphere [7-15].

Compound	m/z	Name	Symbol
	228	bisphenol A	A
	226	4,4'-(cyclopropane-1,1-diyl)diphenol	B
	94	phenol	C
	134	4-isopropenylphenol	D
	136	4-isopropylphenol	E



Scheme S1. The proposed mechanism of EPO/DP reactions in oxygen (O₂) atmosphere.

Table S5. Energy-dispersive X-ray analysis (EDX) elemental composition of the char residue of **EPO**, **EPO2Si**, **EPO_DP2P**, **EPO_DP2P_Mel**, **EPO2Si_DP2P** and **EPO2Si_DP2P_Mel** obtained after the vertical burning test is shown.

Sample	C (wt.%)	O (wt.%)	N (wt.%)	Si (wt.%)	P (wt.%)
EPO	80.1	18.1	1.8	-	-
EPO_DP2P	84.2	11.3	-	-	4.5
EPO_DP2P_Mel	72.1	15.2	2.3	-	10.4
EPO2Si	75.6	15.4	0.7	8.3	-
EPO2Si_DP2P	63.2	26.2	3.4	4.3	2.9
EPO2Si_DP2P_Mel	61.8	21.7	4.1	3.8	8.6

8. Mechanical behavior

Table S6. Results from tensile tests for pure epoxy resin, in-situ silica-epoxy system and the in-situ silica-resin added of melamine and DP (2 wt% of P). The tensile modulus was measured from the slope strain range below 0.2%; all the curves were linear until the breaking point, without plastic deformation.

Sample	E_t (MPa)	$\sigma_{u,t}$ (MPa)	$\epsilon_{f,t}$ (%)	U_T (J/m ³)
EPO	2629 ± 42	112 ± 35	4.2 ± 1.2	2162
EPO2Si	2896 ± 24	89 ± 27	3.1 ± 0.9	1121
EPO2Si_DP2P_Mel	3493 ± 37	72 ± 22	2.1 ± 0.6	590

References

1. X. Liu, K.A. Salmeia, D. Rentsch, J. Hao, S. Gaan, Thermal decomposition and flammability of rigid PU foams containing some DOPO derivatives and other phosphorus compounds, *J. Anal. Appl. Pyrolysis.* 124 (2017) 219–229.
2. K.A. Salmeia, A. Gooneie, P. Simonetti, R. Nazir, J.-P. Kaiser, A. Rippl, C. Hirsch, S. Lehner, P. Rupper, R. Hufenus, Comprehensive study on flame retardant polyesters from phosphorus additives, *Polym. Degrad. Stab.* 155 (2018) 22–34.
3. F. Wang, S. Pan, P. Zhang, H. Fan, Y. Chen, J. Yan, Synthesis and Application of Phosphorus-containing Flame Retardant Plasticizer for Polyvinyl Chloride, *Fibers Polym.* 19 (2018) 1057–1063.
4. W. Zhang, A.A. Dehghani-Sanij, R.S. Blackburn, IR study on hydrogen bonding in epoxy resin–silica nanocomposites, *Prog. Nat. Sci.-Mater.* 18 (2008) 801-805.
5. J.W. Gilman, R.H. Harris, J.R. Sheilds, T. Kashiwagi, A.B. Morgan, A study of the flammability reduction mechanism of polystyrene-layered silicate nanocomposite: Layered silicate reinforced carbonaceous char, *Polym. Adv. Technol.* 17 (2006) 263–271.
6. T. Kashiwagi, F. Du, J. Douglas, K. Winey, H. Jr, J. Shields, Nanoparticle Networks Reduce the Flammability of Polymer Nanocomposites, *Nat. Mater.* 4 (2006) 928–933.
7. D. Braun, W. Von Gentzkow, A.P. Rudolf, Hydrogenolytic degradation of thermosets, *Polym. Degrad. Stab.* 74 (2001) 25–32.
8. H. Yan, C. Lu, D. Jing, X. Hou, Chemical degradation of TGDDM/DDS epoxy resin in supercritical 1-propanol: Promotion effect of hydrogenation on thermolysis, *Polym. Degrad. Stab.* 98 (2013) 2571–2582.
9. K. Shirokane, T. Wada, M. Yoritate, R. Minamikawa, N. Takayama, T. Sato, N. Chida, Total Synthesis of (\pm)-Gephyrotoxin by Amide-Selective Reductive Nucleophilic Addition, *Angew. Chemie Int. Ed.* 53 (2014) 512–516.
10. H. Yan, C. Lu, D. Jing, X. Hou, Chemical degradation of amine-cured DGEBA epoxy resin in supercritical 1-propanol for recycling carbon fiber from composites, *Chinese J. Polym. Sci.* 32 (2014) 1550–1563.
11. S. V Levchik, G. Camino, M.P. Luda, L. Costa, G. Muller, B. Costes, Epoxy resins cured with aminophenylmethylphosphine oxide—II. Mechanism of thermal decomposition, *Polym. Degrad. Stab.* 60 (1998) 169–183.
12. W. Chin, M. Shau, W. Tsai, Synthesis, structure, and thermal properties of epoxy-imide resin cured by phosphorylated diamine, *J. Polym. Sci. Part A Polym. Chem.* 33 (1995) 373–379.

13. M. Shau, T. Wang, Syntheses, structure, reactivity, and thermal properties of new cyclic phosphine oxide epoxy resins cured by diamines, *J. Polym. Sci. Part A Polym. Chem.* 34 (1996) 387–396.
14. W. Zhang, A. Fina, G. Ferraro, R. Yang, FTIR and GCMS analysis of epoxy resin decomposition products feeding the flame during UL 94 standard flammability test. Application to the understanding of the blowing-out effect in epoxy/polyhedral silsesquioxane formulations, *J. Anal. Appl. Pyrolysis.* 135 (2018) 271–280.
15. B. Schartel, Phosphorus-based flame retardancy mechanisms—old hat or a starting point for future development?, *Materials (Basel).* 3 (2010) 4710–4745.